An Intelligent Maximum Power Extraction Algorithm for Inverter-Based Variable Speed Wind Turbine Systems

Quincy Wang, *Member, IEEE,* and Liuchen Chang, *Senior Member, IEEE*

***Abstract*—This paper focuses on the development of maximum wind power extraction algorithms for inverter-based variable speed wind power generation systems. A review of existing maximum wind power extraction algorithms is presented in this paper, based on which an intelligent maximum power extraction algorithm is developed by the authors to improve the system performance and to facilitate the control implementation. As an integral part of the max-power extraction algorithm, advanced hill-climb searching method has been developed to take into account the wind turbine inertia. The intelligent memory method with an on-line training process is described in this paper. The developed maximum wind power extraction algorithm has the capability of providing initial power demand based on error driven control, searching for the maximum wind turbine power at variable wind speeds, constructing an intelligent memory, and applying the intelligent memory data to control the inverter for maximum wind power extraction, without the need for either knowledge of wind turbine characteristics or the measurements of mechanical quantities such as wind speed and turbine rotor speed. System simulation results and test results have confirmed the functionality and performance of this method.**

***Index Terms*—Hill climb searching, maximum power extraction, variable speed wind turbine, wind power generation, wind turbine model.**

I. Introduction

THE INSTALLED wind power capacity in the world has been increasing at more than 30% per year over the past decade [1], [2]. The current surge in wind energy development is driven by multiple forces in favor of wind power including its tremendous environmental, social and economic benefits, the technological maturity, the deregulation of electricity markets throughout the world, public support, and government incentives. Based on a life-cycle assessment [3], the greenhouse gas emission from worldwide electricity generation with the 2000 fuel mix is 0.572 kg of equivalent CO_2 per kWh. In 2000, the total world electricity generation was 14 617 TWh, emitting about 8 364 megatons of equivalent CO_2. Recent developments in wind power generation have provided an economically competitive and technically sound solution to reduce greenhouse gas emissions.

Manuscript received July 18, 2003; revised June 1, 2004. Recommended by Associate Editor M. G. Simoes.

Q. Wang is with Elliott Energy Systems, Inc., Stuart, FL 34997 USA.

L. Chang is with Department of Electrical and Computer Engineering, University of New Brunswick, Fredericton, NB E3B 5A3, Canada (e-mail: lchang@unb.ca).

Digital Object Identifier 10.1109/TPEL.2004.833459

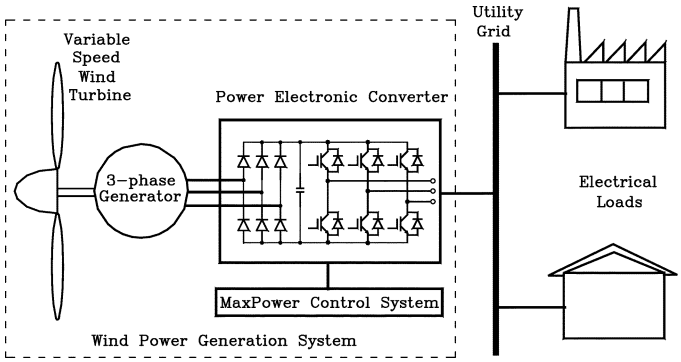

Fig. 1. Typical wind power generation system connected to a utility grid.

Variable speed operation and direct drive generators have been the recent developments in wind turbine drive trains. Compared with constant speed operation, variable speed operation of wind turbines provides 10–15% higher energy output, lower mechanical stress and less power fluctuation. In order to fully realize the benefits of variable speed wind power generation systems (WPGS), it is critical to develop advanced control methods to extract maximum power output of wind turbines at variable wind speeds. A variable speed WPGS needs a power electronic converter, often called an inverter, to convert variable-frequency, variable-voltage power from a generator into constant-frequency constant-voltage power, and to regulate the output power of the WPGS. Traditionally a gearbox is used to couple a low speed wind turbine rotor with a high speed generator in a WPGS. Recently much effort has been placed on the use of a low speed direct-drive generator to eliminate the gearbox [15]. A typical WPGS with a variable-speed direct-drive generator is depicted in Fig. 1.

The mechanical output power at a given wind speed is drastically affected by the turbine's tip speed ratio (TSR), which is defined as the ratio of turbine rotor tip speed to the wind speed. At a given wind speed, the maximum turbine energy conversion efficiency occurs at an optimal TSR [4]. Therefore, as wind speed changes, the turbine's rotor speed needs to change accordingly in order to maintain the optimal TSR and thus to extract the maximum power from the available wind resources.

Previous research has focused on three types of maximum wind power extraction methods, namely TSR control, power signal feedback (PSF) control and hill-climb searching (HCS) control [5]. TSR control regulates the wind turbine rotor speed

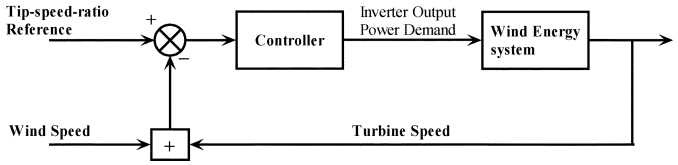

Fig. 2. Block diagram of TSR control.

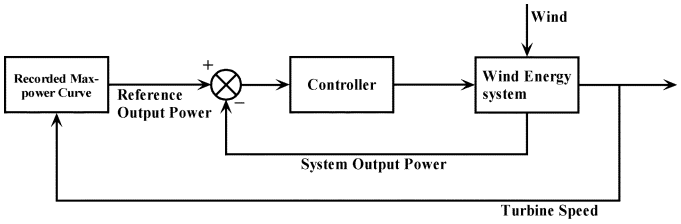

Fig. 3. Block diagram of PSF control.

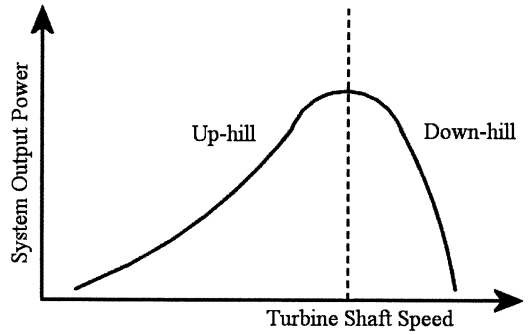

Fig. 4. Principle of hill-climb search control.

to maintain an optimal TSR [6]. As shown in Fig. 2, both the wind speed and turbine speed need to be measured for TSR calculation, and the optimal TSR must be given to the controller. The first barrier to implement TSR control is the wind speed measurement [7], which adds to system cost and presents difficulties in practical implementations. The second barrier is the need to obtain the optimal value of TSR, which is different from one system to another. This dependency on turbine-generator characteristics results in custom-designed control software tailored for individual wind turbines.

PSF control requires the knowledge of the wind turbine's maximum power curve [7]–[10], and tracking of this curve through its control mechanisms, as illustrated in Fig. 3. This maximum power curve needs to be obtained via simulations or tests for individual wind turbines, which makes PSF control difficult and expensive to implement in practice.

To overcome the aforementioned drawbacks, HCS control has been proposed to continuously search for the peak output power of the wind turbine [11]–[14], as shown in Fig. 4. HCS control works well only when the wind turbine inertia is very small so that the turbine speed reacts to wind speed almost "instantaneously." For large inertia wind turbines, the system output power is interlaced with the turbine mechanical power and rate of change in the mechanically stored energy, which often renders the HCS method ineffective.

Equation (1) describes the relationship between the turbine mechanical power $\mathrm{P_m}$, and the electrical system output power $\mathrm{P_{out}}$, where $\mathrm{P_{load}}$ is the load of the turbine; $\mathrm{T_f}$ is the friction torque, ω is the turbine's angular speed, J is the turbine's moment of inertia, and η is the overall electrical efficiency of the system from generator input to inverter output. When J is very small, HCS control can search for a maximum $\mathrm{P_m}$ through $\mathrm{P_{out}}$ regulations. When J is not negligible, HCS control fails to reach the maximum power points under fast wind variations, thus severely limiting the usefulness of this method for large wind turbines

$$P_{\mathrm{m}} = P_{\mathrm{Load}} + T_{\mathrm{f}} * \omega + \omega * J\frac{d\omega}{dt} = \frac{1}{\eta}P_{\mathrm{out}} + T_{\mathrm{f}} * \omega + \omega * J\frac{d\omega}{dt}. \tag{1}$$

It is thus highly desirable to develop a maximum power extraction method for wind turbines, which does not require the measurement of wind speed or turbine rotor speed, is independent of system characteristics, and is applicable to large and small wind turbines. The authors have developed a new intelligent maximum wind power extraction algorithm which meets these criteria.

II. Wind Turbine Model

If the turbine rotor friction is ignored, the mechanical characteristics of a wind turbine can be described by (2)–(5). If the wind speed and the turbine's load power are given, the turbine speed can be solved using these equations and the turbine's $\mathrm{Cp}(\lambda)$ curve which can be obtained by field tests or from design computations

$$T_{\mathrm{m}} - T_{\mathrm{Load}} = Jd\frac{\omega}{dt} \tag{2}$$

$$P_{\mathrm{m}} - P_{\mathrm{Load}} = \omega * Jd\frac{\omega}{dt} \tag{3}$$

$$P_{\mathrm{m}} = C_p(\lambda) * 0.647 * A * u^3 \tag{4}$$

$$\lambda = \frac{r_{\mathrm{m}} * \omega}{u} \tag{5}$$

where $\mathrm{T_m}$—wind turbine mechanical torque; $\mathrm{T_{load}}$—load torque; u—wind speed; A—sweeping area of the turbine rotor; $\mathrm{C_p}$—turbine performance coefficient; λ—tip-speed ratio; $\mathrm{r_m}$—maximum radius of the turbine rotor.

The wind turbine model can be represented as Fig. 5(a) in MATLAB/SIMULINK for simulation studies. This model focuses on the energy transfer characteristics within a wind turbine and does not include the aerodynamic characteristics. Fig. 5(b) shows a typical wind turbine Cp curve obtained through field tests [15]. Designed as a subsystem block in SIMULINK, this model can be easily integrated into the entire wind power generation system along with other components for simulation studies.

III. Advanced Hill-Climb Searching Method

To extend the HCS method into WPGSs with different levels of turbine inertia, advanced hill-climb searching (AHCS) has been proposed by the authors to maximize $\mathrm{P_m}$, through detecting the inverter output power $\mathrm{P_{out}}$ and inverter dc-link voltage $\mathrm{V_{dc}}$. The authors use a diode rectifier to convert the three-phase output ac voltage $(\mathrm{V_{gen}})$ of a generator to $\mathrm{V_{dc}}$. $\mathrm{V_{dc}}$

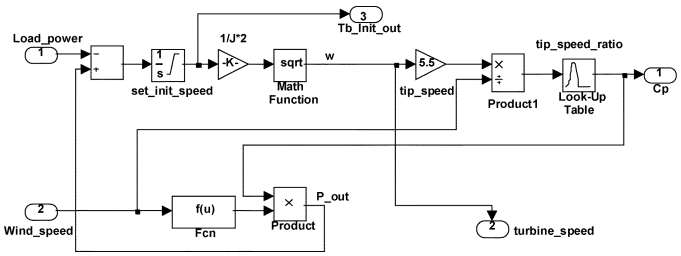

(a)

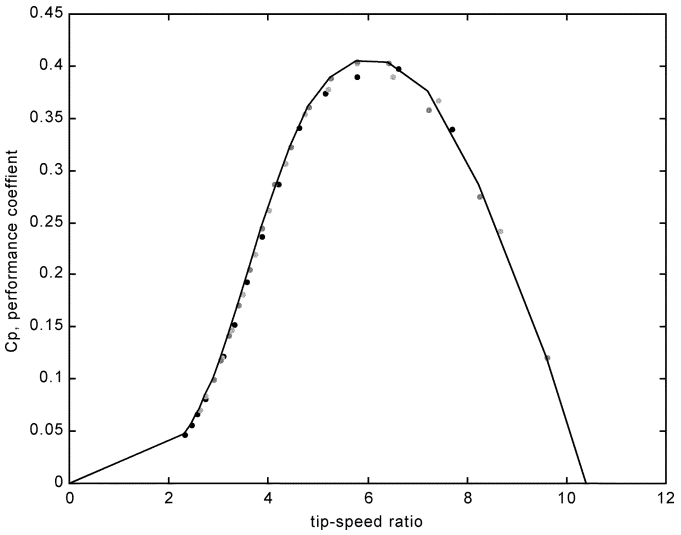

(b)

Fig. 5. (a) Wind turbine model. (b) Cp curve used in the wind turbine model.

TABLE I
JUDGEMENT OF TURBINE MECHANICAL POWER VARIATION

ΔP_{out}	$\Delta(V_{dc}*dV_{dc}/dt)$	ΔP_m	AHCS Action
≥ 0	≥ 0	≥ 0	keep ΔI_{dm}
≤ 0	≤ 0	≤ 0	inverse ΔI_{dm}
> 0	< 0	unknown	$\Delta I_{dm} = 0$
< 0	> 0	unknown	$\Delta I_{dm} = 0$

is related to ω by a function of generator field current $\mathrm{I_f}$ and load current $\mathrm{I_g}$: $\mathrm{V_{dc}} = \mathrm{k(I_f, I_g)} * \boldsymbol{\omega}$. If the sampling period T of the control system is adequately small, the variation of $\mathrm{k(I_f, I_g)}$ can be ignored for the time interval $\mathrm{nT} \leq \mathrm{t} \leq (\mathrm{n}+1)\mathrm{T}$. Thus, $\mathrm{k(I_f, I_g)}$ can be considered as a constant value K during a sampling period. $\mathrm{T_f} * \omega$ and η can also be considered as constant values in the same sampling period.

Based on the above assumptions, the differentiation of (1) is derived as (6) which leads to (7) for digital control purposes. Equation (8) reveals the process to evaluate $\Delta \mathrm{P_{out}}$ and $\Delta(\mathrm{V_{dc}} * \mathrm{dV_{dc}/dt})$ from discrete sampling moments (n) and $(\mathrm{n}+1)$. Thus, the direction of $\Delta \mathrm{P_m}$ can be judged by Table I according to (7). If the direction of $\Delta \mathrm{P_m}$ between (n) and $(\mathrm{n}+1)$ is judged as "unknown", the data from $(\mathrm{n}-1)$, $(\mathrm{n}-2)$ to $(\mathrm{n}-\mathrm{k})$ can also be used to decide the present $\Delta \mathrm{P_m}$ direction. $\Delta \mathrm{P_{out}}$ and $\Delta(\mathrm{V_{dc}} * \mathrm{dV_{dc}/dt})$ can then be calculated by (9) as alternatives. After the direction of $\Delta \mathrm{P_m}$ is detected, the direction of the inverter current demand control signal $\Delta \mathrm{I_{dm}}$, can be decided according to Table I based on the HCS principle. The searching step $\Delta \mathrm{I_{dm}}$ can be selected via experiments or computer simulations. AHCS forms an integral part of the intelligent maximum power extraction algorithm

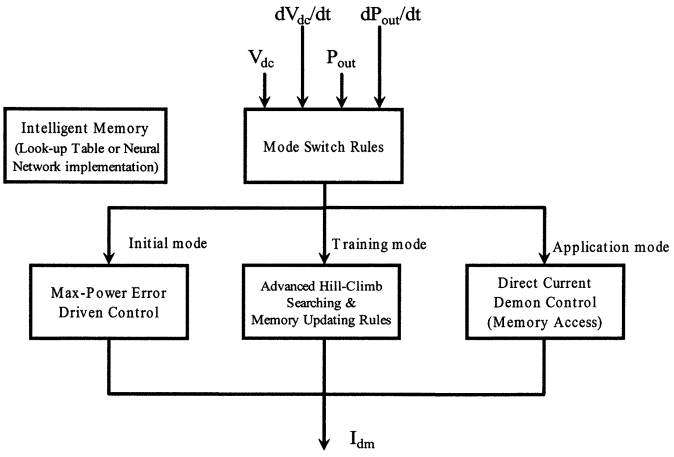

Fig. 6. Structure of the intelligent maximum wind power extraction algorithm.

$$\frac{d}{dt}(P_m) = \frac{1}{\eta} * \frac{d}{dt}(P_{\mathrm{out}}) + JK^2 * \frac{d}{dt}\left(V_{\mathrm{dc}} * \frac{dV_{dc}}{dt}\right) \quad (Given: V_{\mathrm{dc}} = K\omega) \tag{6}$$

$$\Delta P_m = \frac{1}{\eta} * \Delta P_{\mathrm{out}} + JK^2 * \Delta\left(V_{\mathrm{dc}} * \frac{dV_{\mathrm{dc}}}{dt}\right) \tag{7}$$

$$\begin{cases} \Delta P_{\mathrm{out}} = P_{\mathrm{out}}(n+1) - P_{\mathrm{out}}(n) \\ \Delta\left(V_{\mathrm{dc}} * \frac{dV_{\mathrm{dc}}}{dt}\right) = V_{\mathrm{dc}}(n+1) * \frac{dV_{\mathrm{dc}}}{dt}(n+1) \\ \qquad\qquad - V_{\mathrm{dc}}(n) * \frac{dV_{\mathrm{dc}}}{dt}(n) \\ \frac{dV_{\mathrm{dc}}}{dt}(n+1) \approx \frac{V_{\mathrm{dc}}(n+1) - V_{\mathrm{dc}}(n)}{t_{n+1} - t_n} \\ \frac{dV_{\mathrm{dc}}}{dt}(n) \approx \frac{V_{\mathrm{dc}}(n) - V_{\mathrm{dc}}(n-1)}{t_n - t_{n-1}} \end{cases} \tag{8}$$

$$\Delta P_{\mathrm{out}} = P_{\mathrm{out}}(n+1) - P_{\mathrm{out}}(n-k)$$

$$\Delta\left(V_{\mathrm{dc}} * \frac{dV_{\mathrm{dc}}}{dt}\right) = V_{\mathrm{dc}}(n+1) * \frac{dV_{\mathrm{dc}}}{dt}(n+1) - V_{\mathrm{dc}}(n-k) * \frac{dV_{\mathrm{dc}}}{dt}(n-k) \quad (k = 0, 1, 2 \ldots). \tag{9}$$

IV. INTELLIGENT MAXIMUM WIND POWER EXTRACTION ALGORITHM

To provide effective controls to a WPGS under variable wind conditions, direct current demand control (DCDC) applies the recorded search results from AHCS to inverter controls. AHCS and DCDC together form a complete search-remember-reuse process for the intelligent maximum wind power extraction algorithm.

A. Algorithm Description

The structure of the algorithm is shown in Fig. 6. Every execution cycle begins with $\mathrm{V_{dc}}$ and $\mathrm{P_{out}}$ sampling, and calculations of their differentials. Then, mode switch rules will direct the control into one of three execution modes, namely initial mode, training mode, and application mode. Regardless of which mode the algorithm chooses, the inverter current demand $(\mathrm{I_{dm}})$ will be calculated in that mode and fed to the inverter to regulate the system output power. The controller repeats the above process to update continuously the current demand. $\mathrm{I_{dm}}$ is defined as the requested peak value of the sinusoidal inverter output current.

When the intelligent memory is empty for the present V_{dc} and the system is in transient states, mode switch rules switch the system control into initial mode, where initial I_{dm} values are determined by max-power error driven (MPED) control (see Section IV-B). When the system is in steady states, mode switch rules switch the system control into training mode, where AHCS is applied for I_{dm} calculation in a search process. Meanwhile, memory updating rules are evaluated to fill the trained data into the empty part, or to optimize the existing part of the intelligent memory. Training mode acts as a nonlinear system optimizer with on-line training capability. When the system is in transient states and the intelligent memory has a current demand data corresponding to a V_{dc} value, application mode is activated for fast I_{dm} determination by direct current demand control (DCDC).

Large I_{dm} variations caused by discrete selections of three different control modes have been eliminated to avoid algorithm instability. To obtain $I_{dm}(n+1)$ from $I_{dm}(n)$, both initial mode and training mode calculate I_{dm} variation only, ΔI_{dm}, which is a small limited value. In application mode, I_{dm} is calculated based on intelligent memory data obtained in training mode, thereby providing a seamless transition from training mode. When transferring from initial mode to application mode at the very beginning before the intelligent memory is fully established, ΔI_{dm} is mandatorily limited by the program to avoid sudden I_{dm} jumps. Both system simulation and laboratory tests have proved that the algorithm is stable between mode switches. No large I_{dm} change nor large generator voltage and current changes were observed.

The principle behind this algorithm is a "search-remember-reuse" process. The algorithm will start from an empty intelligent memory with a relatively poor initial performance. During the execution, training mode will use the searched data by AHCS to gradually train the intelligent memory to record the training experience. The algorithm will reuse the recorded data in application mode for fast execution. This "search-remember- reuse" will repeat itself until an accurate memory of system characteristics is established. Therefore, after the algorithm is adequately trained, its power extraction performance is optimized. Since the intelligent memory is trained on-line during system operation, such a process is also referred as "on-line training process."

B. Max-Power Error Driven Control (MPED) in Initial Mode

MPED provides the system with a preliminarily optimized operating point when the intelligent memory is empty. The control reference signal of MPED controller is the maximum system output power, which can only be reached when the wind speed is sufficiently high. At an arbitrary wind speed, the MPED controller is designed to keep the error between the maximum power and the present output power as small as possible.

The flow chart of the MPED method is shown in Fig. 7, where P_{max} is the maximum system output power, err is power error signal, P_{sign} and I_{dm_sign} are variables to identify the directions of err and I_{dm} variations, respectively, I_{dm_step} is the step length of I_{dm} variation. The method intends to adjust I_{dm} to reduce the power error, with a fixed step length I_{dm_step}. Basically, MPED method extends the regular HCS method into wind energy conversion systems.

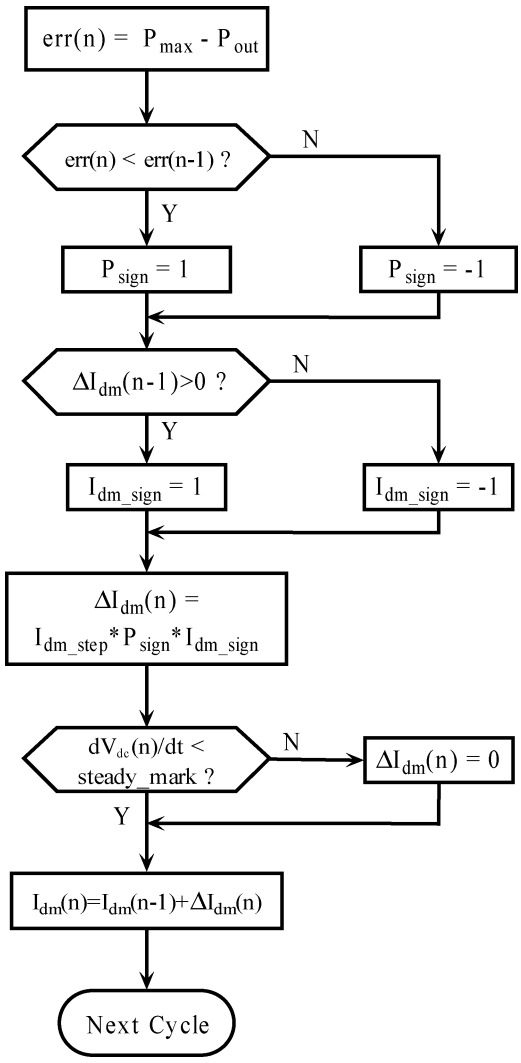

Fig. 7. Flow chart of MPED control.

C. Intelligent Memory and Memory Updating Rules

The intelligent memory records the system max-power points and the corresponding control variables at different operating conditions. Depending on the system structure, the control variables of a wind power generation system may include the inverter output current demand I_{dm} for output power control, generator excitation current for generator output voltage control, control demand for dc link voltage etc. If I_{dm} is the only control variable for output power regulation and V_{dc} is the only index referring to operating condition as in the case of most small variable speed wind turbines, a lookup table can be used to construct the intelligent memory.

Table II shows the structure of a lookup table implementation for the intelligent memory, where P_{dm} is the system output power demand. The table is derived from simulation studies of a 10-kW wind energy conversion system with a three-blade horizontal axis wind turbine. The first column (V_{dc}) contains dc-link voltage as the index of the lookup table. The second column (P_{dm}) is the highest system output power recorded at a particular V_{dc}. The third column (I_{dm}) is the corresponding current demand sent to the inverter to obtain the maximum power.

TABLE II
LOOKUP TABLE IMPLEMENTATION OF THE INTELLIGENT MEMORY

V_{dc}	P_{dm}	I_{dm}
76	0	70
101	64.8	70
126	226	66.6
151	390.4	60.8
176	619.9	58.2
201	926.9	53.1
226	1317.4	47.1
251	1808.5	47.6
276	2409	44.2
301	3124.1	39.7
326	3976.4	31.9
351	4966	28.6
376	6110.4	35.9
401	7415.6	43.6
426	8894.8	52.3
451	10558.4	62.1
476	11775.3	69.2
501	11902.4	70
550	12000	70

In training mode, $\mathrm{P_{out}}$ will be compared with $\mathrm{P_{dm}}$ at the nearest $\mathrm{V_{dc}}$ in the table, and the contents of the table will be updated if the present $\mathrm{P_{out}}$ is larger than $\mathrm{P_{dm}}$ in the lookup table. This updating process will repeat continuously until the maximum $\mathrm{P_{dm}}$ points for every $\mathrm{V_{dc}}$ value is fully recorded, forming the system's maximum power curve. Data updating rules in training mode consist of three rules, which need to be satisfied at the same time before updating the intelligent memory. Mathematically expressed as (10), **Rule One** requests the system to be at steady state for data updating. In (10), Steady_mark is a small value representing steady state. The reason for Rule One is that, at transient states, turbine mechanical max-power points cannot be detected through $\mathrm{P_{out}}$ observation due to the effect of turbine inertia

$$\left|\frac{dV_{\mathrm{dc}}}{dt}\right| \leq \text{Steady\_mark.} \tag{10}$$

Rule Two requests that the system be running in the down-hill region (see Fig. 4), which ensures the wind turbine operate in the stable operation region. Rule Two is expressed as (11). The first two equations in (11) present an increasing $\mathrm{P_m}$ as seen in (7). If the third equation of (11) can also be satisfied, the system is then operating in the down-hill region and thus ready for data updates

$$\begin{cases} \Delta P_{\mathrm{out}} \geq 0 \\ \Delta\left(V_{\mathrm{dc}} * \frac{dV_{\mathrm{dc}}}{dt}\right) \geq 0 \\ \frac{dV_{\mathrm{dc}}}{dt} < 0 \end{cases}. \tag{11}$$

Expressed as (12), **Rule Three** is to replace the existing data in the intelligent memory with the data corresponding to higher power. This rule forces the data in memory to be updated toward the max-power curve of the wind turbine system

$$P_{\mathrm{out}} > P_{\mathrm{dm}}. \tag{12}$$

The objective of intelligent memory updating is to search and record the system's max-power curve (i.e., $\mathrm{P_{out\_max}} - \mathrm{V_{dc}}$ curve) when the system is in steady states.

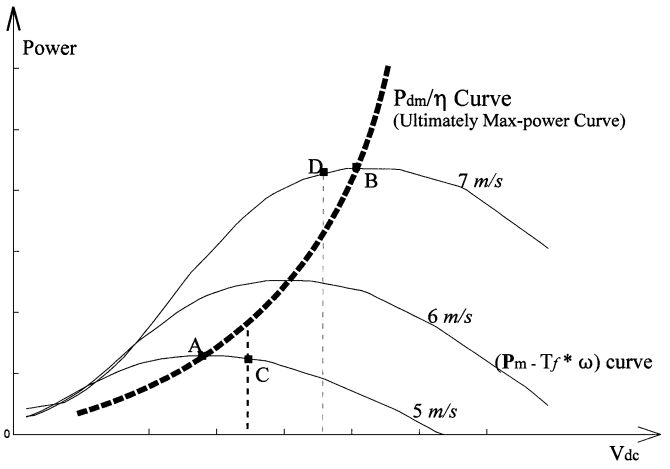

Fig. 8. DCDC principles.

D. Direct Current Demand Control in Application Mode

Mode switch rules activate application mode when the system is in transient states and the data in the intelligent memory is available for the present dc-link voltage. Intelligent memory records the $\mathrm{I_{dm}} - \mathrm{V_{dc}}$ relationship optimized for max-power extraction at variable wind speeds, as described by (13). DCDC utilizes this recorded relationship to determine the $\mathrm{I_{dm}}$ value based on the present dc-link voltage $\mathrm{V_{dc}}$. From the definition of $\mathrm{I_{dm}}$, the inverter output power, i.e., the WPGS output power can be expressed as (14), where $\mathrm{V_{grid}}$ is the grid voltage, N is the number of phases of the grid. $\mathrm{K(V_{dc}, I_{dm})}$ of (14) is the current waveform coefficient, which is equal to one when the output current is sinusoidal. For quasisinusoidal current waveforms due to insufficient dc-link voltage, $\mathrm{K(V_{dc}, I_{dm})}$ is a constant between zero and one, and is determined by $\mathrm{V_{dc}}$ and $\mathrm{I_{dm}}$ for a chosen inverter PWM strategy.

By submitting (13) into (14), $\mathrm{P_{out}}$ can be determined by $\mathrm{V_{dc}}$ and can thus be simply treated as a function of $\mathrm{V_{dc}}$, as represented by $\mathrm{P_{dm}(V_{dc})}$ in (15). Submitting (15) to (1), (16) is derived

$$I_{\mathrm{dm}} = f(V_{\mathrm{dc}}) \tag{13}$$

$$P_{\mathrm{out}} = N * K(V_{\mathrm{dc}}, I_{\mathrm{dm}}) * \frac{I_{\mathrm{dm}}}{\sqrt{2}} * V_{\mathrm{grid}} \tag{14}$$

$$\begin{aligned} P_{\mathrm{out}} &= N * K\left(V_{\mathrm{dc}}, f(V_{\mathrm{dc}})\right) * \frac{f(V_{\mathrm{dc}})}{\sqrt{2}} * V_{\mathrm{grid}} \\ &= \frac{N * V_{\mathrm{grid}}}{\sqrt{2}} * \left[K\left(V_{\mathrm{dc}}, f(V_{\mathrm{dc}})\right) * f(V_{\mathrm{dc}})\right] \\ &= P_{\mathrm{dm}}(V_{\mathrm{dc}}) \end{aligned} \tag{15}$$

$$(P_m - T_f * \omega) - \frac{1}{\eta} * P_{\mathrm{dm}}(V_{\mathrm{dc}}) = \omega * J * \frac{d\omega}{dt}. \tag{16}$$

Because the intelligent memory is optimized for max-power extraction, the $\mathrm{V_{dc}}$ based $1/\eta * \mathrm{P_{dm}(V_{dc})}$ curve can be illustrated as the dash line of Fig. 8, which is close to and ultimately will be the turbine's max-power curve. The solid lines of Fig. 8 illustrate the turbine output power curve, i.e., $(\mathrm{P_m} - \mathrm{T_f} * \omega)$ versus $\mathrm{V_{dc}}$ at different wind speeds. Assuming the system is running at point C at a wind speed of 5 m/s, DCDC will use the $\mathrm{V_{dc}}$ at

TABLE III
WIND SYSTEM SPECIFICATIONS

Items	10kW System	50kW System
Turbine Type	3-blade Horizontal Axis, variable speed turbine	2-blade Vertical Axis, variable speed turbine
Sweeping Area	32 m^2	147 m^2
Turbine Inertia	76.8 $kg.m^2$	7500 $kg.m^2$
Generator Coupling	direct coupling	direct coupling
Generator	10kW 3-phase permanent magnet synchronous generator	50kW 3-phase direct-drive synchronous generator
Inverter	10kW 1-phase grid- connected IGBT inverter	100kW 3-phase grid-connected IGBT inverter
System Grid Voltage	240 V AC	480 V AC (line-line)

point C to find a corresponding I_{dm} based on the data recorded in the intelligent memory as per (13), to control the inverter output power following (14). The inverter output P_{out} will be equal to the recorded P_{dm}, and the $1/\eta * P_{dm}(V_{dc})$ will be a point on the dash-line curve corresponding to the present V_{dc}. Because this dash-line point is higher than turbine's mechanical power P_m at point C, the left side of (16) will be negative. The turbine will then slow down until reaching point A, which is eventually the max-power point at the wind speed of 5 m/s.

Therefore, DCDC will force the system to operate at the intersection points of the turbine power curve and the dash line, which is recorded in the intelligent memory after initial optimization and is updated in training mode to become eventually the system max-power curve with the highest Cp value at any wind speed.

V. SIMULATION RESULTS

Simulations on the max-power extraction algorithm are conducted based on two different WPGS models. One is a 10-kW Bergey EXCEL wind turbine system model, with a permanent magnet synchronous generator and a single-phase IGBT inverter. The other is a 50-kW vertical axis wind turbine system model, with a 50-kW direct-drive synchronous generator and a three-phase IGBT inverter. The specifications of these two systems are listed as Table III. The WPGS models are first established using SIMULINK block sets, and the max-power algorithm is written in the MATLAB program.

For a practical wind turbine, the best Cp is about 0.4 where the maximum wind power is extracted [4]. Based on the developed maximum power extraction algorithm, Fig. 9(a) shows the progress of average Cp of the 10-kW system when the wind speed changes randomly between 2 m/s and 14 m/s every 150 s, while Fig. 9(b) shows that of the 50 kW system. From these two figures, the average Cp is relatively low at the initial stage. After a certain time, the algorithm is able to gradually search for better operating points. Correspondingly, the turbine's average Cp is continuously improved. For the 10-kW system with small turbine inertia, the algorithm can reach and maintain thereafter an average Cp of 0.39 after 500 min of on-line training. For the 50-kW system with large turbine inertia, the necessary training time is longer.

Fig. 9 demonstrates that the proposed max-power extraction algorithm is suitable for both small inertia and large inertia wind turbine systems, and the algorithm is able to extract the maximum available wind energy after a sufficient period of training.

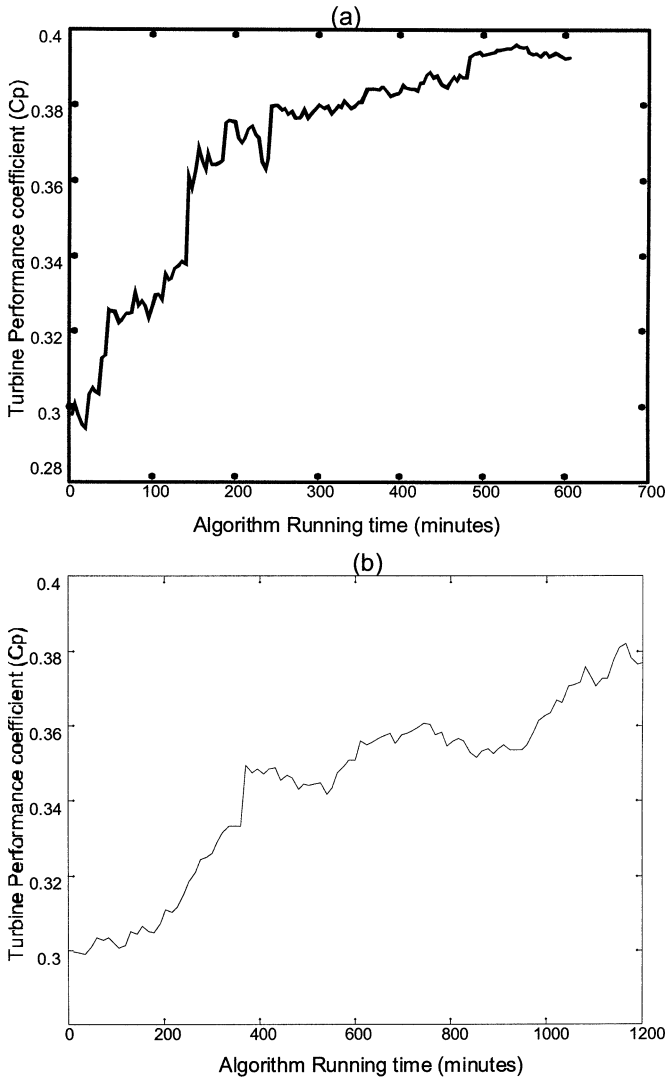

Fig. 9. Average Cp progress curve. (a) 10-kW system. (b) 50-kW system.

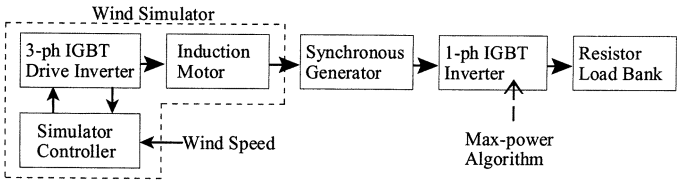

Fig. 10. Laboratory test environment.

VI. LABORATORY TEST RESULTS

A. Wind Turbine Simulator System [16]

The intelligent maximum wind power extraction algorithm has been implemented and tested in our research laboratory. The test environment is shown as Fig. 10, where a wind turbine simulator system is used as the prime mover to drive a synchronous generator in replacement of a real wind turbine [16]. A single-phase IGBT inverter is used to extract the generator output energy and to feed to a resistor load bank. The max-power algorithm is implemented in the microcontroller system of the single-phase inverter.

A variable speed induction motor drive system is developed to simulate characteristics of real wind turbines. The wind tur-

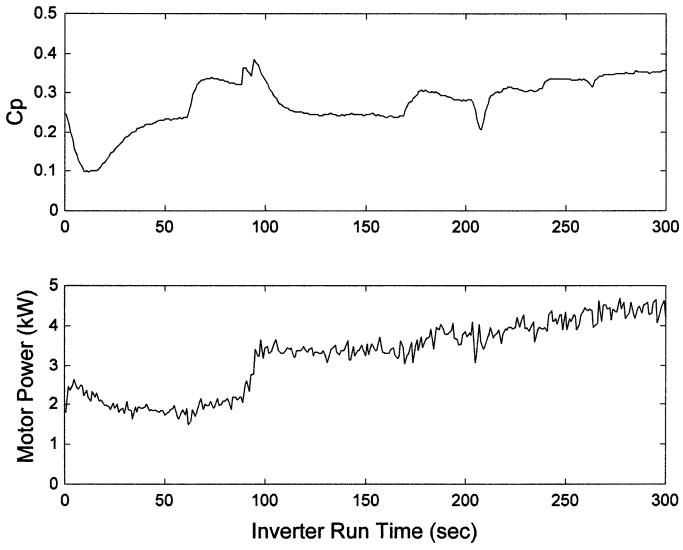

Fig. 11. Searching performance without online training.

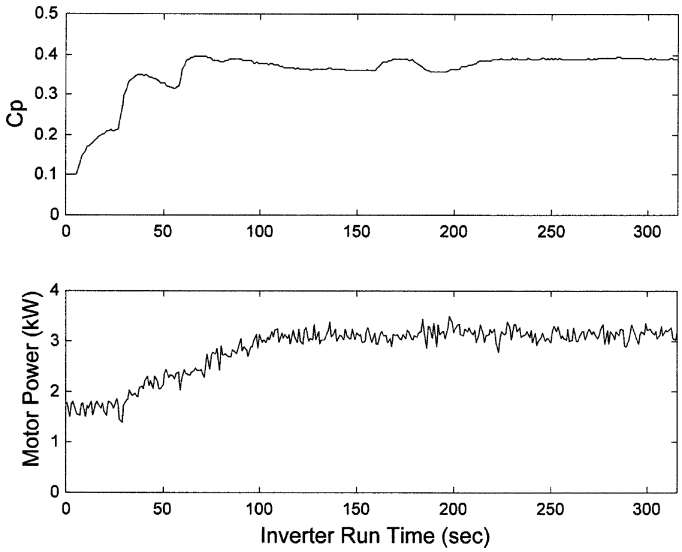

Fig. 12. Searching performance with 2 h of online training data available at the beginning of the search.

bine simulator controller accepts the motor torque and speed as feedback signals, calculates current and frequency demands of the three-phase drive inverter based on the dynamic wind turbine model presented in Section II, and exports these demand signals to a drive inverter to form a close-loop control. The drive inverter then controls the induction motor to generate shaft torque like a real wind turbine. The wind simulator controller can automatically generate wind speed variations according to a measured wind profile, or set a fixed wind speed for bench testing.

B. Performance Tests of the Max-Power Algorithm

Various laboratory tests have been conducted based on the developed maximum power extraction algorithm. The performance of the algorithm was first tested and evaluated with and without the online training process. Fig. 11 shows the test results without online training, under a constant wind speed set at 6 m/s. After the startup period, the inverter begins to search for optimal points for max-power extraction. The searching process is shown in this figure, as depicted by the gradual increase in both Cp and motor power (i.e., wind turbine mechanical power). However, without the on-line training, the searching progress is slow. The high Cp region of about 0.4 has not been reached after 340 s of searching. In a real wind turbine environment, a constant wind speed can rarely last for 340 s. This test proves the necessity of online training as an integral part of the developed max-power extraction algorithm. Fig. 12 shows the test results after the algorithm has received two hours of online training, at a constant wind speed of 5 m/s. The test data show faster searching process and Cp achievement than those of Fig. 11.

C. Dynamic Tests for Variable Wind Speeds

The dynamic response of the developed algorithm at variable wind speeds has been tested after the system has received two hours of online training. Fig. 13 shows the test results with the wind speed changing from 3 to 5 m/s. The system initially operated at a wind speed of 3 m/s and then step-changed to 5 m/s. It can be observed from Fig. 13 that the transition time for the algorithm to reach new steady state with high Cp once again is about 125 s.

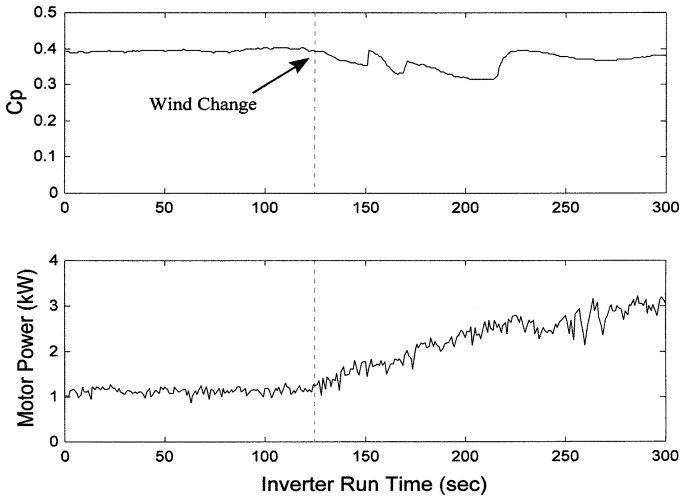

Fig. 13. Dynamic test results with 2 h of online training data available at the beginning of this test.

VII. Conclusion

This paper focuses on the development of maximum wind power extraction algorithms for inverter-based variable speed WPGS. Existing max-power extraction algorithms have been briefly reviewed. WPGS models have been established by the authors for simulation studies. The advanced hill-climb searching method has been proposed in this paper for maximum power searching in wind systems with various turbine inertia. AHCS is independent of system hardware characteristics, and thus has overcome the difficulties of the previous hill-climb searching methods caused by wind turbine inertia. Without a need for measurements of wind speed and turbine rotor speed, AHCS is simple to implement.

To further improve the dynamic performance of AHCS, the intelligent maximum wind power extraction algorithm has been developed. By recording in an intelligent memory the search results of AHCS through an on-line training process, the algorithm can record the optimum system operating conditions, and then use DCDC to find the max-power points rapidly and effectively.

Computer simulation has been conducted for two wind power generation systems, a 10-kW Bergey wind turbine system with a single-phase inverter, and a 50-kW vertical axis wind turbine system with a three-phase inverter. The functionality and performance of the proposed intelligent max-power extraction algorithm have been verified. The intelligent max-power algorithm has been successfully implemented in a single-phase IGBT inverter for wind energy conversion systems. Laboratory test results based on a wind simulator system have further confirmed the effectiveness of the developed maximum wind power extraction algorithm.

REFERENCES

[1] P. Gipe, "Soaring to new heights: the world wind energy market," *Renewable Energy World*, vol. 5, no. 4, pp. 33–47, Sept./Oct. 2002.

[2] M. Jujawa, "Large wind rising," *Renewable Energy World*, vol. 6, no. 2, pp. 39–51, Mar./Apr. 2003.

[3] L. Gagnon, *Comparing Electricity Generation Options: Greenhouse Gas Emissions*. Montreal, QC, Canada: Hydro Quebec, Jan. 2003.

[4] G. L. Johnson, *Wind Energy Systems*. Englewood Cliffs, NJ: Prentice-Hall, 2003.

[5] I. K. Buehring and L. L. Freris, "Control policies for wind energy conversion systems," *Proc. Inst. Elect. Eng. C*, vol. 128, pp. 253–261, Sept. 1981.

[6] T. Thiringer and J. Linders, "Control by variable rotor speed of a fixed-pitch wind turbine operating in a wide speed range," *IEEE Trans. Energy Conv.*, vol. EC-8, pp. 520–526, Sept. 1993.

[7] M. Ermis, H. B. Ertan, E. Akpinar, and F. Ulgut, "Autonomous wind energy conversion systems with a simple controller for maximum-power transfer," *Proc. Inst. Elect. Eng. B*, vol. 139, pp. 421–428, Sept. 1992.

[8] R. Chedid, F. Mrad, and M. Basma, "Intelligent control for wind energy conversion systems," *Wind Eng.*, vol. 22, no. 1, pp. 1–16, 1998.

[9] R. Hilloowala and A. M. Sharaf, "A rule-based fuzzy logic controller for a PWM inverter in a stand alone wind energy conversion scheme," *IEEE Trans. Ind. Applicat.*, vol. IA-32, pp. 57–65, Jan. 1996.

[10] R. Chedid, F. Mrad, and M. Basma, "Intelligent control of a class of wind energy conversion systems," *IEEE Trans. Energy Conv.*, vol. EC-14, pp. 1597–1604, Dec. 1999.

[11] M. G. Simoes, B. K. Bose, and R. J. Spiegal, "Fuzzy logic-based intelligent control of a variable speed cage machine wind generation system," *IEEE Trans. Power Electron.*, vol. PE-12, pp. 87–94, Jan. 1997.

[12] ——, "Design and performance evaluation of a fuzzy-logic-based variable-speed wind generation system," *IEEE Trans. Ind. Applicat.*, vol. IA-33, pp. 956–964, July/Aug. 1997.

[13] T. Tanaka and T. Toumiya, "Output control by Hill-Climbing method for a small wind power generating system," *Renewable Energy*, vol. 12, no. 4, pp. 387–400, 1997.

[14] J. H. Enslin and J. V. Wyk, "A study of a wind power converter with micro-computer based maximum power control utilizing an over-synchronous electronic Scherbius cascade," *Renewable Energy*, vol. 2, no. 6, pp. 551–562, 1992.

[15] Q. Wang, "Maximum wind energy extraction strategies using power electronic converters," Ph.D. thesis, Univ. New Brunswick, Fredericton, NB, Canada, June 2003.

[16] L. Chang, R. Doraiswami, T. Boutot, and H. Kojabadi, "Development of a wind turbine simulator for wind energy conversion systems," in *Proc. IEEE Canadian Conf. Electrical and Computer Engineering (CCECE'00)*, Halifax, NS, Canada, May 2000, pp. 550–554.

Quincy Wang (S'98–M'02) received the B.Sc. and M.Sc. degrees from Northern Jiaotong University, Beijing, China, in 1991 and 1994, respectively, and the Ph.D. degree from the University of New Brunswick, Fredericton, NB, Canada, in 2003, all in electrical engineering.

He is currently a Senior Power Electronics Lead Engineer with the R&D Department, Elliott Energy Systems, Inc., Stuart, FL, working on power electronic inverter development for distributed power generation systems with micro-turbine engines.

Liuchen Chang (S'87–M'92–SM'99) received the B.S.E.E. degree from Northern Jiaotong University, Beijing, China in 1982, the M.Sc. degree from the China Academy of Railway Sciences (CARS), Beijing, in 1984, and the Ph.D. from Queen's University, Kingston, ON, Canada, in 1991.

From 1984 to 1987, he was at CARS as a Researcher on railway traction systems. He is currently a Professor of electrical and computer engineering and NSERC Chair in Environmental Design Engineering at the University of New Brunswick, Fredericton, NB, Canada. He has published over 90 papers in technical journals and conference proceedings and two books. His principal research interests and experience include distributed power generation, renewable energy conversion, analysis and design of electrical machines, variable-speed drives, finite-element electromagnetic analysis and design, power electronics, and electric vehicle traction systems.